CO₂ sensitivity studies under laboratory and outdoor conditions as contribution to climate change discussions

Matthias Marvan[1]; Christoph Marvan[2]; Martin Steiner[3]; Ernst Hammel[4]

[1)]m.marvan@gmx.at; [2)] c.marvan@gmx.at [3)] steiner@str2030.at [4)] ernst.hammel@yahoo.com

ICR Independent Climate Research, *2344 Maria Enzersdorf, Austria*

The EU considers climate change as an existential threat and wants to reduce net greenhouse gas emissions by at least 55% by 2030 and down to 0% by 2050 within the "EU Green Deal" and economic growth should be decoupled from the use of energy resources. It therefore sees fighting climate change as one of the most important targets[1].

There is considerable dis-consensus about growing CO_2 levels in terms of temperature increase and their implications on living conditions. While the IPCC and the EU are predicting strong and negative effects some experts[2,3] have shown that there are considerable flaws in the basic models, data and impact scenarios.

With a low cost experimental setup we measured the IR backradiation from varying CO_2 levels within a given N_2 atmosphere. The results confirm previous findings about an infrared CO_2 saturation within the earth atmosphere. Measurements were also performed studying potential thermal forcing of additional CO_2 against clear night skies. These results and their interpretation should be seen as another contribution to the general discussion about correct climate measures to be taken.

I. Introduction

The Earth's atmosphere is mainly composed of the diatomic molecules, dinitrogen, N_2, and dioxygen, O_2; 78.08% and 20.95% by volume respectively. They are radiatively inactive. The remaining 0.97% is made up from argon (0.93%), carbon dioxide, (CO_2 0.04%), and traces of hydrogen, helium, and other "noble" gases (by volume), methane, nitrous oxide and ozone, but generally a variable amount of water vapor is also present, on average about 1% at sea level. Greenhouse [GH] molecules are those that absorb terrestrial IR radiation, that which is emitted by the Earth's surface as a result of the warming effect of incoming solar radiation. Their absorption characteristics allow them to act in the retention of heat in the atmosphere and to ensure that the global mean temperature of the atmosphere is tolerable to life – the so called "greenhouse effect". The more important compounds are water vapor, carbon dioxide, methane, dinitrogen monoxide (nitrous oxide), and ozone, in decreasing order of effectiveness, mainly because of their concentrations.

The infrared (IR) spectra of CO_2 as the main GH gas over a 100 meters path length is presented in Figure 1 by plotting the transmission of the gas against the wavenumber, $1/\lambda = v/c$ (λ = wavelength, v = frequency, c = velocity of light). The transmission T (also referred as transmittance) is the extent by which the incident radiation at any wavenumber is transmitted by the sample; If all the radiation is absorbed T = 0, if none is absorbed T = 1.

According to Kirchhoff's law absorptivity A and transmittance T in a reflection free medium are related by A=1-T . The same law allows us also to propagate the equality of the long wave emissivity ε and absorptivity a_{lw}.
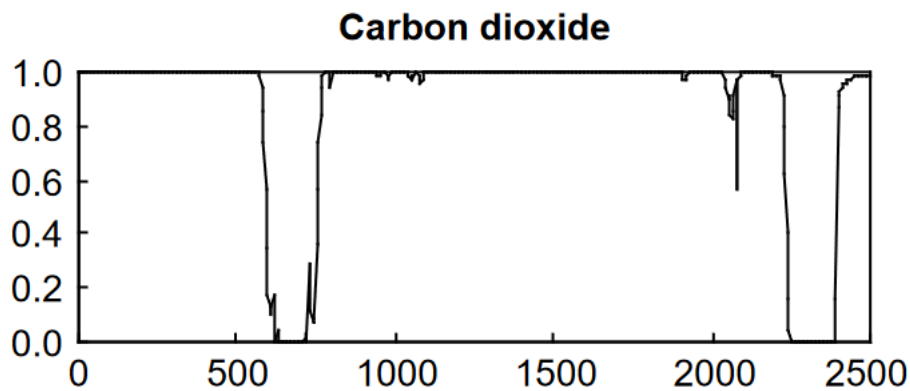
Carbon dioxide

Fig.1 CO_2 IR Transmittance over 100 meters against wavenumber generated from HITRAN [4]

The CO_2 spectrum is dominated by the bending vibration, centered at 667 cm^{-1} (= 14.992 µm) and the asymmetrical stretching mode at 2349 cm^{-1} (= 4.257 µm) The extra very weak bands arise from further excitations and represent very small absorptions that are very often claimed to be significant in calculating the GH effect accurately.

The Earth's surface has a mean global temperature of 288 K and its emission is approximated by a blackbody at that temperature, consisting of continuous radiation unlike that of the GH gases which is specific to each molecule and made up from discrete rotational or rotation-vibrational bands. The continuous Planck (or blackbody) surface radiance is shown by the blue curve in Figure 2, together with the absorption bands of the main GH gas CO_2.
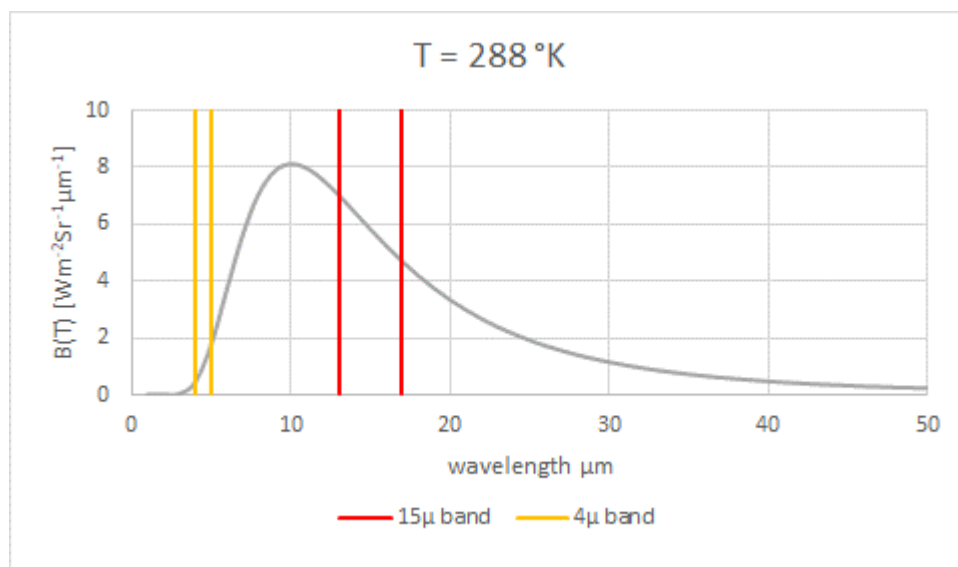

Figure 2: Black body radiator at T=288 °K and major CO_2 absorption bands

The contribution of the 15μm and the 4μm CO_2 band to the total black body IR absorption can be estimated by integration of Fig.1 with a rough maximum of 25 %, where the major contribution comes from 15μm.

The Solar irradiance that is intercepted by our atmosphere is $\pi a^2 S_0$, where a is the earth radius. A fraction α (the "planetary albedo") is reflected back to space. The remaining portion is absorbed. Averaging over a long time and over the total area of the globe, the absorbed solar radiation has to be in balance with the radiation emitted by the atmosphere. In a very simplified 2D model we get according to Stefan-Boltzmann

$$(1-\alpha)\frac{S_0}{4} = \sigma T_E^4 \qquad (1)$$

where T_E is the "emission temperature". Assuming that α=0.3, we find from T_E =255 °K, a temperature is much lower than the observed global average surface temperature of T_S =288 °K. That means that the natural greenhouse effect heats additional ΔT_{GH} = 33 °K, corresponding to

$$\sigma T_S^4 - \sigma T_E^4 = 150 \, W/m^2 \qquad (2)$$

Applying these values to the Planck function for an average surface temperature of 15 °C (288°K) gives the following energy values for the respective absorption bands:

13.26 - 17.07 μm (15μ band), energy density 9.21554 x 10^{-7} J/m³, being 17.58% of the total emission and a photon density of 6.948 x 10^{13} photons per m³,

4.189 - 4.377 μm (4μ band), energy density 5.723 x 10^{-9} J/ m³, being 0.109% of the total emission and a photon density of 1.220 x 10^{11} photons per m³.

From above considerations we see that only the 15μ band is significant with an IR absorption limited to 0.1758 x 391 W/m² = 69 W/m² *and back-radiation to 69/2 = 34.5 W/m²* even less than our first estimation from figure 2. Simplified energy balance considerations in a single atmospheric layer are sketched in the following drawing.
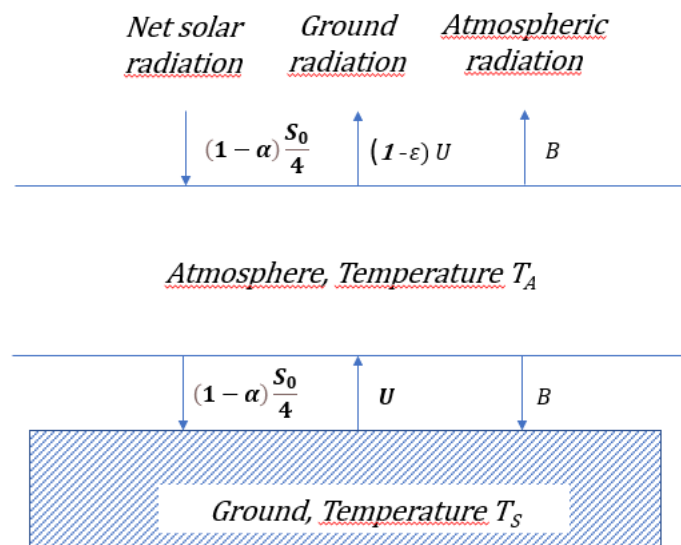

Figure 3: Single-layer model of the atmosphere. *S* is the Solar irradiance; α is the albedo of the ground (0.05-0.2 for water-covered ground; 0.1-0.4 for bare ground; 0.1-0.25 for vegetated ground; 0.5-0.9 for snow-covered ground); *U* is the terrestrial radiation, of which a fraction (1-ε) penetrates directly through the

atmosphere to space; B is the radiation emitted by the atmosphere[5].

With $\varepsilon = 1$ we get

$$\sigma T_S^4 = U = 2\sigma T_A^4 = 2\sigma T_E^4 \qquad (3)$$

and

$$T_S = \sqrt[4]{2} \cdot T_E \qquad (4)$$

With T_E =255 °K we therefore obtain T_S =303 °K. This value is considerably higher than the observed 288 °K. The discrepancy between theory and observation is explained by the fact that the atmosphere is not totally opaque to long-wave radiation. The presence of the atmosphere raises the temperature at the Earth's surface considerably. This effect is referred to as the "greenhouse effect". We assume now that the atmosphere is "semi-grey", i.e. it absorbs a constant fraction ε of the long-wave radiation, but is still transparent to solar radiation and emits (upwards and downwards) at a rate given by

$$B = \varepsilon\sigma T_A^4 = \frac{\varepsilon}{2-\epsilon}\sigma T_E^4 \qquad (5)$$

Where σT_A^4 is the radiation energy content of atmosphere. This leads to

$$T_S = \sqrt[4]{\frac{2}{2-\epsilon}} \cdot T_E \qquad (6)$$

With ε =0.78, we then obtain T_S = 288 °K. We can conclude that in this simplified model only 22% or 42,8 W/m² of the IR radiation is escaping to space and a net power balance of 152 W/m² - as expected from (2) - get permanently recycled as part of the backscattered radiation. From the indicated major CO_2 bands in Fig.2 we get

$$\varepsilon_{CO2} = 0.25 \ \varepsilon \ = 0.2$$

For more appropriate multilayered atmospheres we can take over the picture from the American Chemical Society
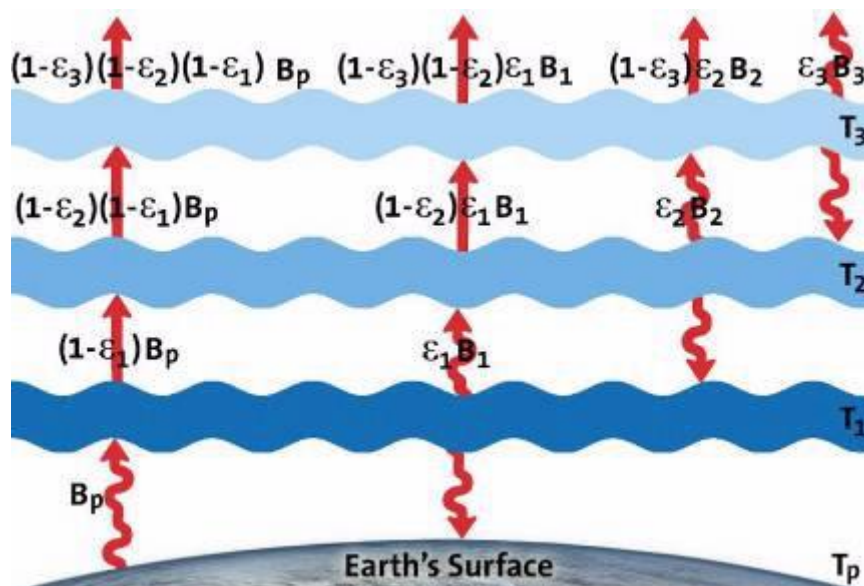

Figure 4: The multilayer atmosphere model is illustrated here for a three-layer atmosphere[6].

Instead of using layered-atmosphere models there exist excellent empirical formulas to be used. Night skies are shielded by clouds and humidity against radiation-loss, while clear and dry conditions cannot compensate for strong radiation-losses. This has been studied e.g. by the modified Swinbank model[7,8]

$$P_{SB} = (1 + KC^2) \cdot 8{,}78 \cdot 10^{-13} \cdot T_S^{5{,}852} \cdot RH^{0{,}07195} \qquad (7)$$

where

P_{SB} upwards and downwards directed atmospheric radiation in W/m^2
K = 0.34 clouds < 2 km, 0,18 for 2 km < altitude < 5 km, 0,06 for > 5 km
C = Cloud cover (0 clear skies, 1 covered skies)
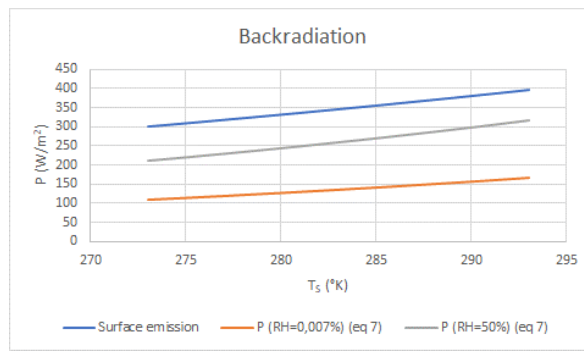T = temperature in °K
RH = relative humidity in %

Figure 5. The effect of humidity on backward radiation compared between RH=0.007% and RH=50%. The blue line is the surface radiation at emissivity $\varepsilon_S \cong 0.95$ according to Stefan-Boltzmann

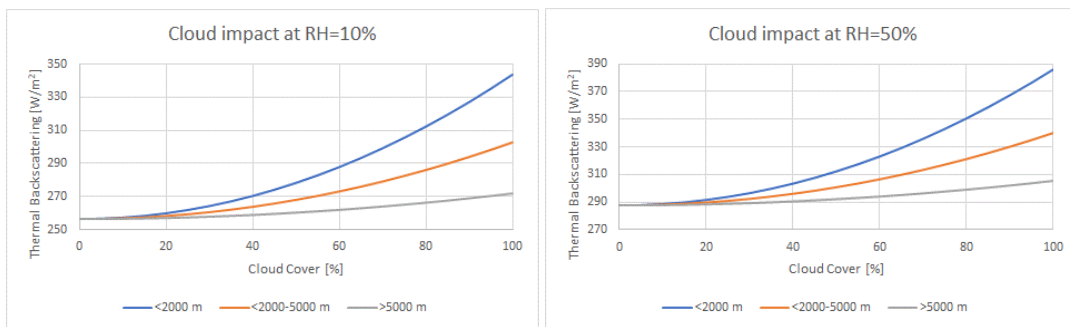Humidity has a strong impact and cloud coverage has even stronger impact on the back-radiation.

Figure 6. Thermal backward radiation characteristics of cloudy skies at RH=10% and RH=50%.

The last figures suggest indeed that climate predictions depend critically on values like average relative humidity, cloud coverage and albedo. These values vary considerably over the surface, depending on local temperature and geographic details. Gridded computer models can account for such values over years of observations to a certain extent only. Instabilities and risks due to feedback loop mismodelling and/or negligence of external geo- or astrophysical influences are obvious.

Data from ground measurements (Fig. 7) indicate that the downward (backward) radiation of the atmosphere shows indeed full saturation the IR CO_2 bands
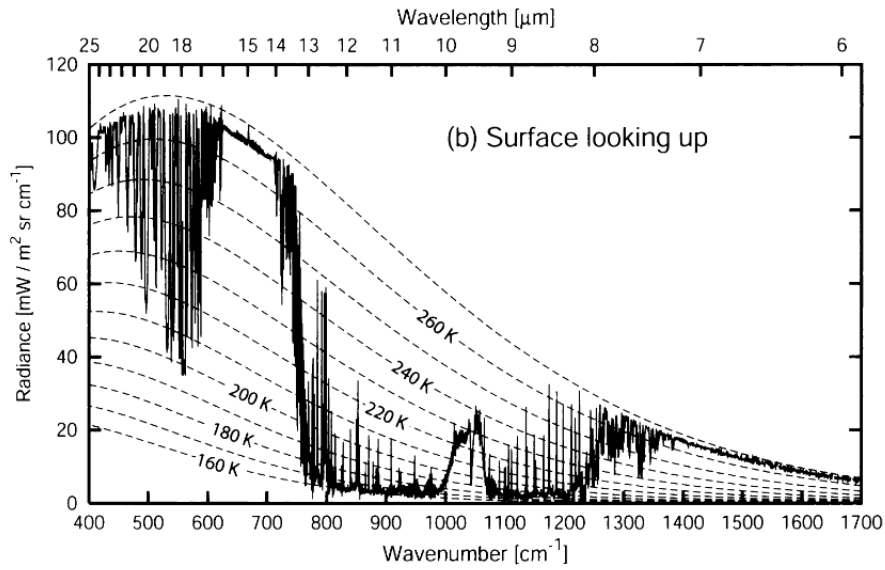
Figure 7: Measurements[9] of the infrared emission spectrum of the cloud-free atmosphere at the arctic surface looking upward.

and does not support noticeable additional Thermal Forcing (TF) by increasing CO2 in the lower atmosphere. It shows almost complete saturation of the 15μ central peak and close-to-saturation of the surrounding 15μ band edges. Early studies[10]
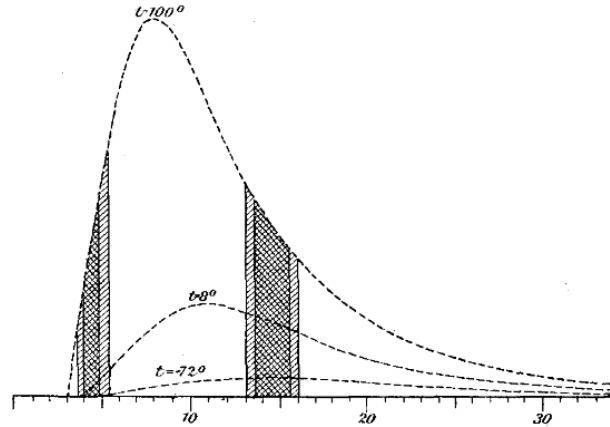

Figure 7: Studies of J. Koch at the Physical Department of Knut Angström[10]

concluded as well that TF will not be significantly influenced by further increase of atmospheric CO_2. On the other side it is well known that concentrations below 20% of the current level would be detrimental to plant growth and climate.

The wavelength dependent absorption a_λ and re-emission is calculated from Beers Law, where transmission is exponentially reduced by increasing absorber thickness L

$$a_\lambda(L) = 1 - t_\lambda(L) = 1 - \frac{I_\lambda(L)}{I_\lambda(0)} = 1 - e^{-k(\lambda,L)} \quad (8)$$

Kirchhoff's law requires that absorbed radiation should get emitted again, or in other words absorptivity should equal emissivity. For a limited wavelength window $\Delta\lambda$ the specific emissivity $\varepsilon_{\Delta\lambda}(L)$ is therefore obtained by

$$\varepsilon_{\Delta\lambda}(L) = \frac{\int_{\lambda_1}^{\lambda_2} I_\lambda(0).a_\lambda(L)\,d\lambda}{\int_0^\infty I_\lambda(0)\,d\lambda} \qquad (9)$$

Where the spectral extinction coefficients a_λ is be obtained from HITRAN or other databases.

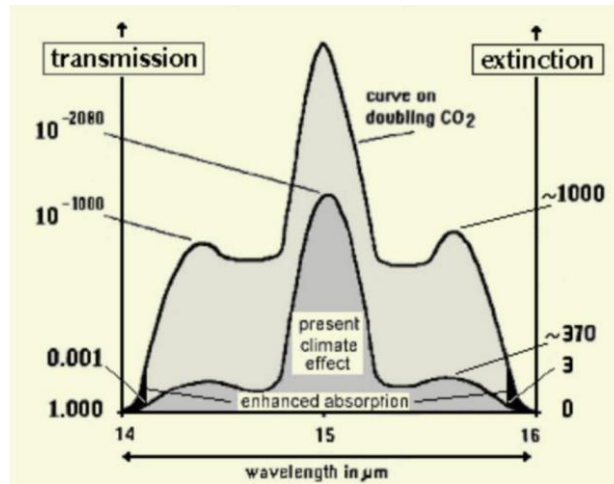There are arguments about the significance of the unsaturated edges in 15 µ band.

Figure 8 : Transmission and Extinction Ratios of the 15 µ band.

With extinction < 3 they contribute only 0,17% to the full 15 µ band, when we consider their respective integrals. This has also been shown by Howard[11] used further down in this study.

The infrared (IR) spectra of the four main GH gases over a path length of 100 meter are presented in Figure 9, their concentrations being those that pertain to the atmosphere at sea-level which amounts to 45% humidity.
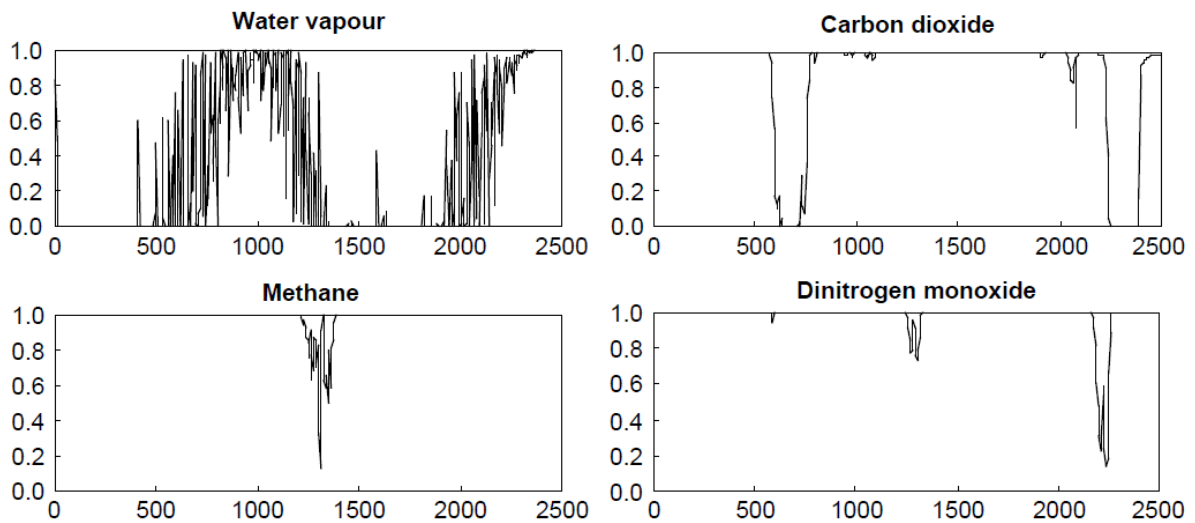

Figure 9 : Infrared spectra of the main greenhouse gases as calculated using the HITRAN data base; Transmission is plotted against wavenumber (cm^{-1})[9]

Alone the 0 - 500 cm^{-1} band of H_2O at 45% RH absorbs 66% of the IR radiation. The $1300 - 1800$ cm^{-1} band absorbs another 1%.

In an 8,2 km thick atmosphere of 1 bar pressure, we can calculate the equivalent thickness of the CO2 content at approximate current levels of 400 ppm. If we apply this to various atmospheric layers, we obtain the following table,

H [m]	M(z)/M	1-M(z)/M	L_{CO2}^{up} [cm]	L_{CO2}^{down} [cm]
0	0	1	344,83	0,00
500	0,06893722	0,93106278	321,06	23,77
1000	0,1331221	0,8668779	298,93	45,90
5000	0,51045834	0,48954166	168,81	176,02
10000	0,76034896	0,23965104	82,64	262,19
20000	0,94256738	0,05743262	19,80	325,03
30000	0,98623621	0,01376379	4,75	340,08
40000	0,99670149	0,00329851	1,14	343,69
∞	1	0	0,00	344,83

Table 1: equivalent of 400 ppm atmospheric CO_2 in meter at 1 bar atmospheric pressure

where we obtained the altitude dependent masses M from the barometric formula

$$\frac{M[z]}{M} = 1 - e^{-\frac{z}{H}} \qquad (10)$$

and H=7 km. The total mass below the altitude z is calculated as

$$M(z) = \int_0^z \rho(z')\, dz' = \rho(0)H \left(1 - e^{-\frac{z}{H}}\right) \qquad (11)$$

The thickness of the CO_2-layer L_{CO2} is a calculated value for a standard atmosphere at 1013.25 hPa and a total weight of 5.13×10^{15} tons of 8.21 km air at current 420 ppm. The table helps to understand the order of magnitudes when studying atmospheric greenhouse effects by CO_2. It also illustrates that 75% of the total CO_2 is contained within the troposphere below 10 kms altitude and 95% are below 20 kms. *If we were to concentrate all the CO2 (at 400ppm) of an 8.2km thick atmosphere with a pressure of 1bar in a single column, the height of the column would be around 3.5m.* The optical path length of CO_2 IR radiation at these conditions is below 1 cm and therefore we can expect full saturation already at 420 ppm. From thermodynamics we obtain

$$\frac{dT}{dz} = \frac{\gamma-1}{\gamma} mg \,/\, R \qquad (12)$$

where $\gamma = \frac{c_P}{c_v}$ (e.g. 7/5 for dry air) , m = 29 g/mol and R is the gas constant. For the International Standard Atmosphere with $\gamma = 1.26$ we obtain $\frac{dT}{dz} = -6.5\,°K/km$. Using this formula we can estimate the LW back-radiation at higher altitudes, when substituting the $T_S \rightarrow T_S - \frac{dT}{dz} \times \Delta z$.
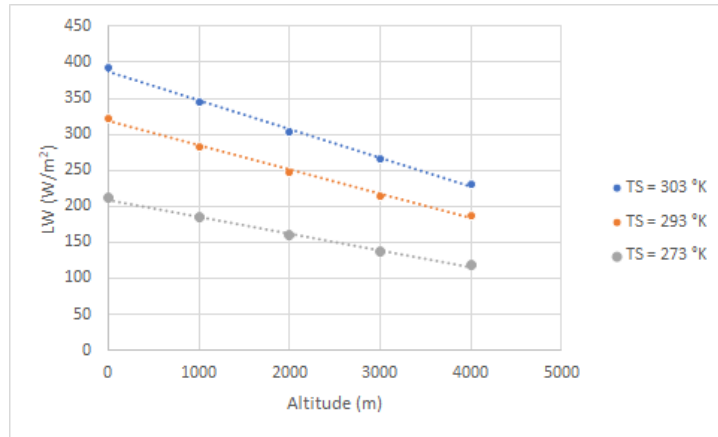
Figure 10: estimated back-radiation in Standard Atmosphere at three different surface temperatures

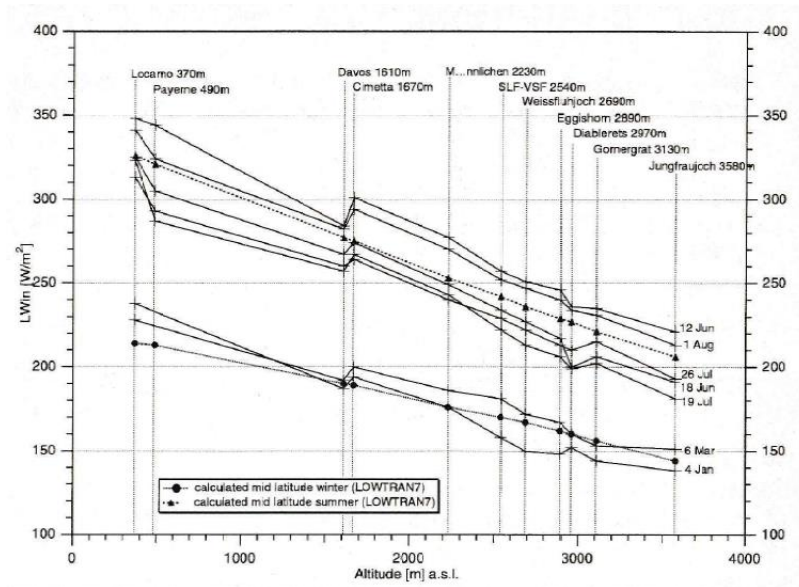This might be compared to measurements taken by a group from ETH Zurich in 1998

Figure 11: Altitude dependence of back-radiation with courtesy from C. Fröhlich [12]

The absorptivity *a* can be calculated using Beer's law for an infrared radiator from eq. 8 in a more generalized form.

$$a(c,L) = 1 - t(c,L) = 1 - \frac{I(c,L)}{I(c,0)} = 1 - e^{-k.c.L} \qquad (13)$$

From Akram [13] we can obtain k = 1,82x10⁻⁶ppm⁻¹cm⁻¹ to calculate *a* as function of L
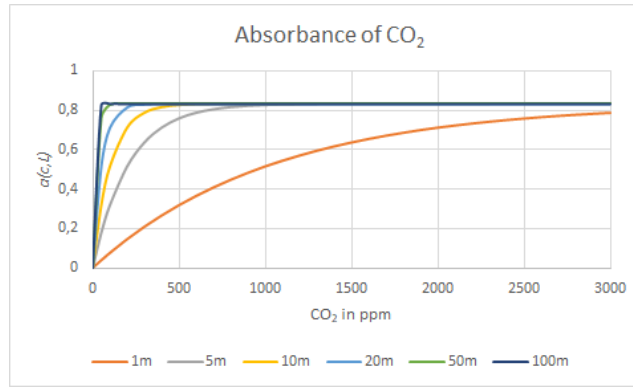
Figure 12: absorbance of EMIRS200 IR light source in CO_2 from [13]

Figure 12 shows IR absorption saturation at current CO_2 levels already at air column length below 20 m. From this simple model we must conclude that other mechanisms than CO_2 increases explain TE effects in the total energy budget.

Howards[11] parameterizes total absorption of strong lines at 15µm and 4.3µm according to

$$\int A_v \, dv = C + D \log w + K \log(p + P) \qquad (14)$$

and

$$\bar{A} = \frac{\int A_v \, dv}{v_2 - v_1} \qquad (15)$$

Substituting these values for $v_2 - v_1 = 250 \; cm^{-1}$ in the 15µm band and $v_2 - v_1 = 340 \; cm^{-1}$ for the 4.3µm band we obtain for a standard atmospheric layer of 1 km
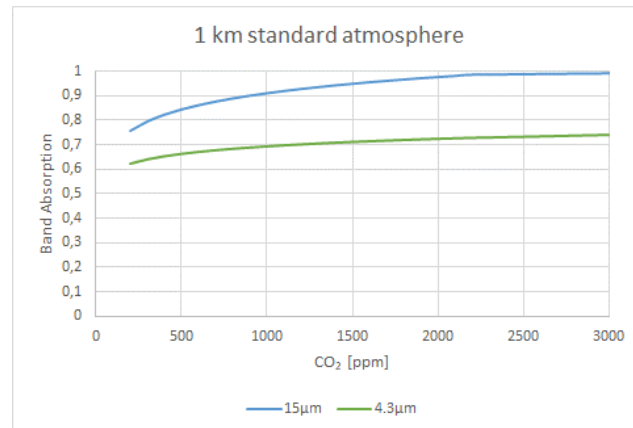

Figure 13: Band absorption within 1 km standard atmosphere[11]

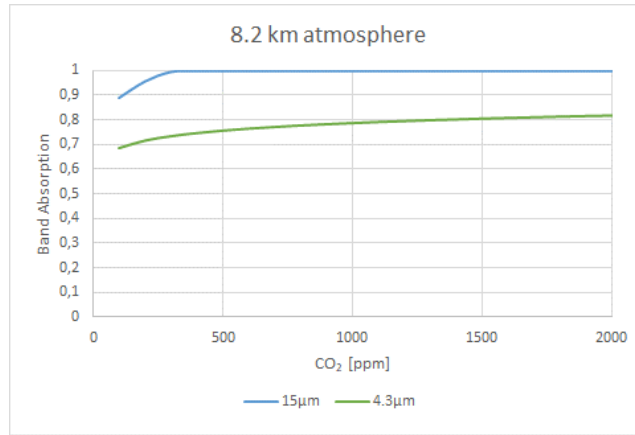and for 8.2 km thick atmosphere as used for table 1

Figure 14: Band absorption within a 8.2 km atmosphere[11]

Howard defines the band limits for 15µm by 500-800 cm^{-1} and for 4.3µm by 2160-2500 cm^{-1}. Applying these values to the Planck black body curve in Fig.1 gives radiation ratios for these values of 32% and 3% respectively. Using these ratios, we obtain the contributions to the total absorption of the atmosphere for variable CO_2 concentrations
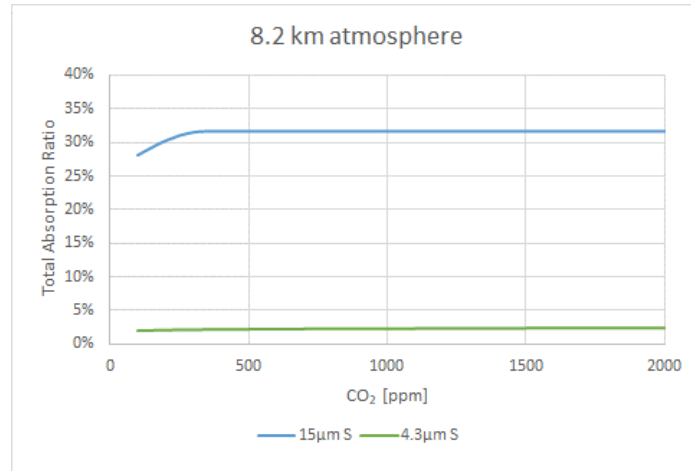

Figure 13: Absorption ratios for the two strong CO_2 absorption bands according to ref.[11]

An increase from 400 to 800 ppm in CO_2 shows no measurable increase in IR absorption for the 15µ and 4.3µ bands and therefore total saturation. Other elaborate studies[14] estimate the total terrestrial long wavelength absorptivity a_{LW}

$$a(L) = \frac{\int_0^\infty I_\lambda(0) \cdot a_\lambda(L) \, d\lambda}{\int_0^\infty I_\lambda(0) \, d\lambda} \times 100\% \quad (16)$$

and obtain the following results for different latitudes

CO2 (ppm)	absorptivities ε (%)				
	tropics	mid-latitudes	high- latitudes	average 3 zones	global mean
0	81.90	69.44	58.98	74.68	77.02
35	83.80	74.48	67.04	78.43	80.08
70	84.18	75.35	68.32	79.10	80.62
140	84.65	76.31	69.80	79.86	81.29
210	84.99	77.00	70.77	80.40	81.76
280	85.28	77. 51	71.52	80.83	82.14
350	85.53	77.95	72.14	81.19	82.45
380	85.65	78.12	72.38	81.34	82.58
420	85.76	78.33	72.68	81.51	8274
490	85.91	78.67	73.16	81.80	83.00
560	86.16	78.98	73.61	82.06	83.24
630	86.35	79.29	74.02	82.32	83.46
700	86.52	79.58	74.41	82.56	83.68
770	86.69	79.85	74.78	82.79	83.88

Table2: Calculated a_{LW} from Harde[14] for various CO_2 concentrations

Th next figure shows the global mean values of the table above. While our previous model neglected the layered structure by assuming an isobar atmosphere, Harde[14] was taking the barometric effects into account.
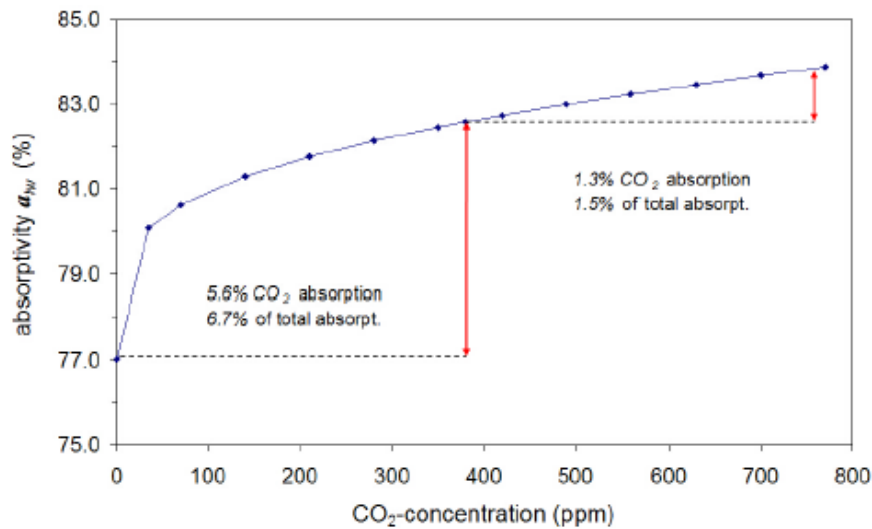

Figure 15: Influence of CO_2 concentration and doubling on total absorptivity from Harde[14]

This study shows an upper limit of additional TE by 1.5%. Average surface temperatures of $T_S = 288°K$ correspond to 390 Wm^{-2} black body radiation. From the foregoing considerations we learned that doubling CO_2 atmospheric concentrations from 400 to 800 ppm amount to maximum 1,5% change of energy absorbed in the atmosphere, i.e. maximal 3 Wm^{-2} of back-radiation increase. Using the Stefan-Boltzmann formula we then obtain a first estimation of a corresponding temperature increase or GH contribution of 0.5 °K by having 800 ppm atmospheric content compared to the current 400 ppm. This corresponds also very well to the results from Wijngaarden and Happer[2]
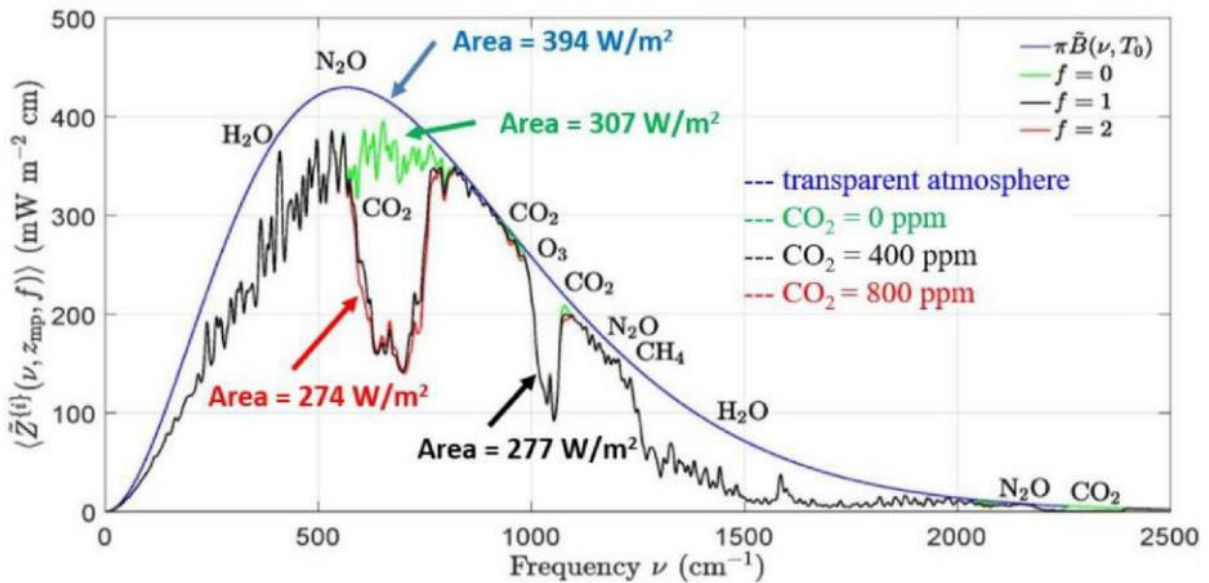
Figure 16: Total atmospheric absorptivity changes by CO_2 increases calculated by Wijngaarden and Happer[2]

Ground measurements (Fig.7) fall in line as well and indicate almost complete saturation of IR absorption in our atmosphere. We were therefore interested to design a simple and independent low-cost experimental setup to demonstrate this saturated behavior. This setup and the results obtained will be described in the following section.

II.   Experimental Methods

The aim of this work was therefore to demonstrate in a simple manner that an IR-active gas can indeed influence the heat radiation of a body. Another aim was to demonstrate that CO_2 back-radiation is limited by saturation of absorbance. This was realized by two different experimental setups.

The measurements should allow us to learn if the saturation behavior measured by others and discussed in the foregoing sections of this work are indeed correct and draw conclusions towards the question of CO_2-induced global warming.

According to the second law of thermodynamics heat flows from hotter to colder objects ("downhill"), unless energy in some form is supplied to reverse the direction of heat flow or there is a medium which absorbs part of the energy and isotropically reemits like it, like it is believed happening within our atmosphere. Our test atmospheres were studied against a -25°C cooled black disc ("Lab Mode") or a cloudless night sky ("Outdoor Mode") using natural day or night IR sources.

Thermal Forcing was measured using a S401C IR Sensor from Thorlabs ® . It is useful for the wavelength range from 190nm – 20 μm and provides an optical power working range from 10μW – 1W. Resolution is specified with 1μW and measurement uncertainty with ± 3%.

Figure 16 explains the setups for Lab and Outdoor Modes. In Fig. 16a ("Lab Mode") a cooling compression device is placed below a black disc. The measurement cylinder covered by a thin

Polyethylene (PE) foil is mounted airtight by proper silicone seals. On the opposite and upper side a KBr Window glass is directed towards the laboratory ceilings. The IR detector is mounted in the center of the KBr window. The back-radiation is measured by using a IR sensor from Thorlabs [®].
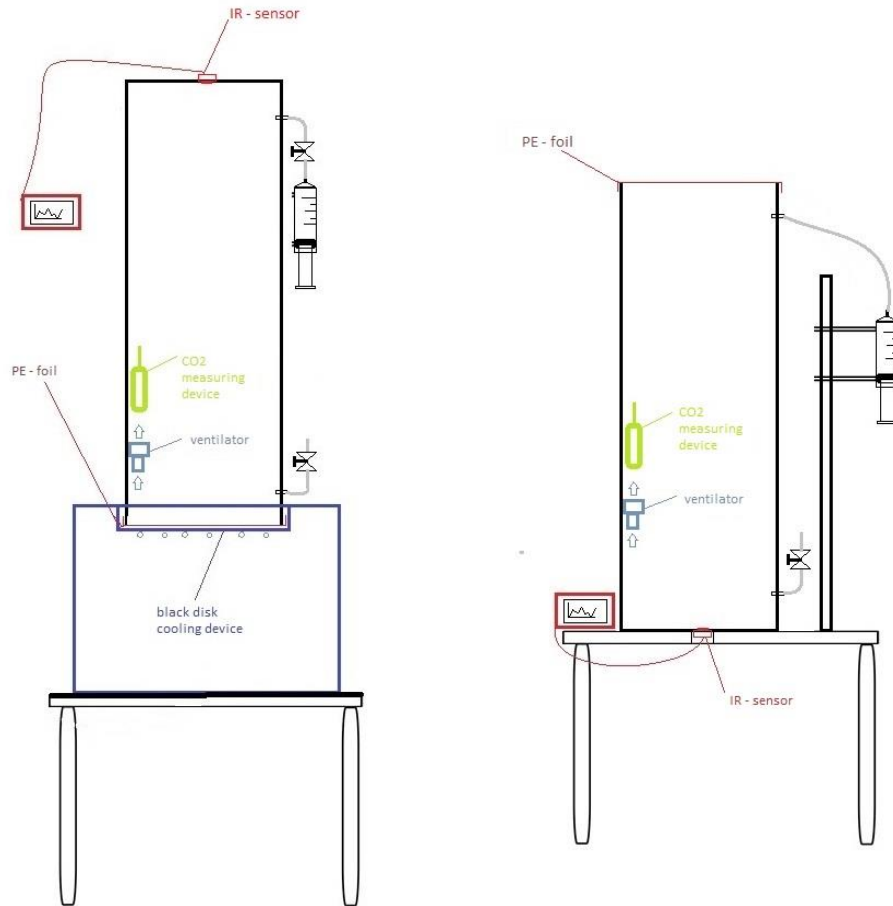

Figure 17: experimental setup for (a) "Lab Mode" using a cooling compressor and (b) "Outdoor Mode"

Translating these setups into energy flow diagrams like in Figs. 3 and 4 we obtain for 17a
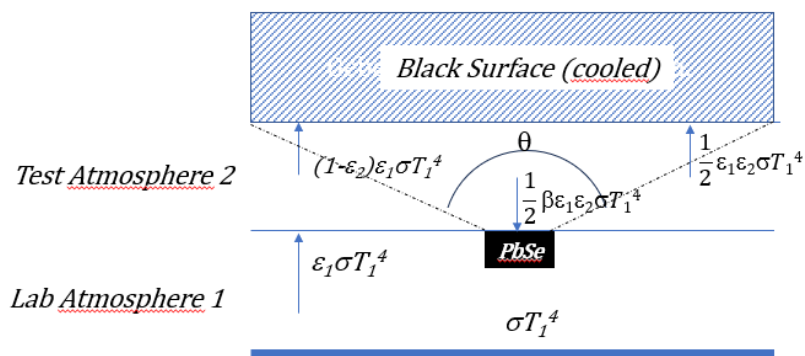
Figure 18: "Lab Mode" test bench with cooled black disc.

 As shown in Fig. 18 the "Lab Mode" IR sensor response is solely determined by the back-radiation from Test Atmosphere 2 with increasing CO_2 concentrations. The cold plate on the other side of the test cylinder allows thermal flow according to the second law of thermodynamics. Inside the volume of the test cylinder a CO_2 detector and a low-power ventilator are mounted and run by a combined power pack. The communication with the CO_2 detector is performed via Bluetooth. β is the intensity ratio $\beta = A_D \sin^2 \theta$ for an IR detector with numerical aperture θ within the cylindrical test column and the detector area A_D of 1 cm². ε_2 solely depends on the GH gas concentrations in the test tube and the intensity $\frac{\beta}{2}\epsilon_1\epsilon_2\sigma T_1^4$ is measured by a PbSe IR detector from Thorlabs®.

In the "Outdoor Mode (Fig. 17b) the test cylinder is rotated by 90°, the cooling compressor is removed and replaced by the clear night sky. The temperature gradient in this case is the difference between T_S and T_E, where T_E is derived from (7)

$$T_E = 4\sqrt{\frac{(1+KC^2)\cdot 8,78 \cdot 10^{-13}\cdot T_S^{5,852}\cdot RH^{0,07195}}{\sigma}} \qquad (17)$$
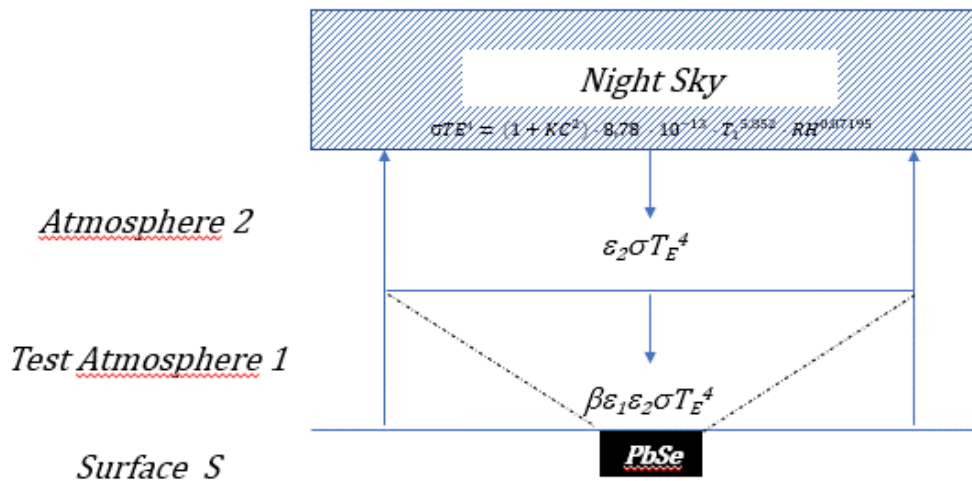

Figure 19: Experimental " Outdoor Mode" during clear night skies

The down-dwelling radiation through the test chamber into the IR detector is determined by

$$P = \beta\varepsilon_1\varepsilon_2\sigma T_E^4 \qquad (18)$$

Using the parametrization of Howard[11] we obtain for CO_2 test atmospheres power densities below the detection limit of the IR sensor of 10μW/cm² . Using stronger GH gases would in fact significantly raise ϵ_1 as we have tested in our experimental series. This would prove that CO_2 is a relatively weak greenhouse gas even when increasing its concentrations into the percentage region, compared to other GH gases, which would be detectable already at relatively low concentrations.

III.   Results

The 7 liter test cylinder in figure 17 a was filled up with pure nitrogen. CO2 was added in 50 ml steps. Simultaneously the CO_2 detector was used to measure the concentration while the ventilator was trying to homogenize the gas volume admixture. In Fig. 20 the obtained power values of the IR-detector are plotted
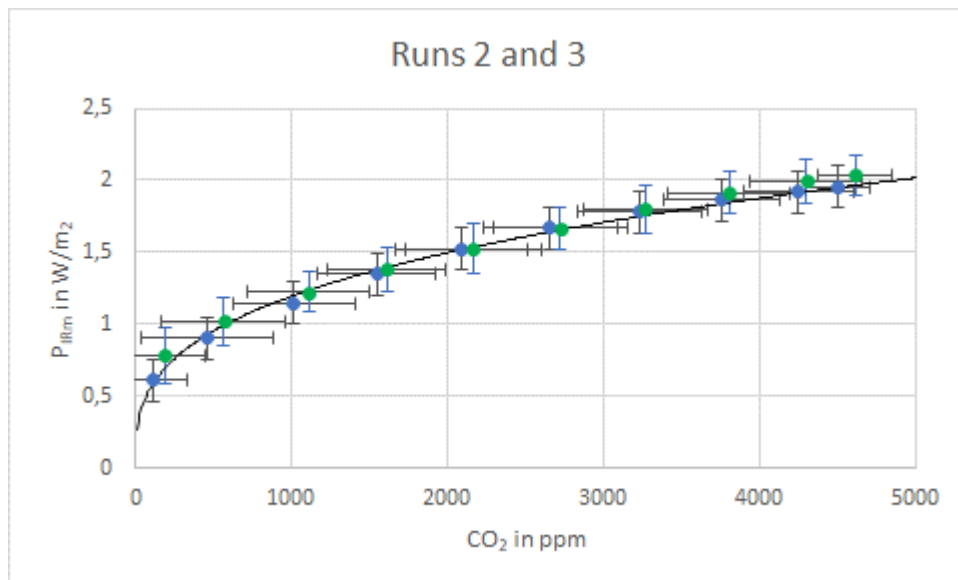

Figure 20: Run 2.2 and Run 2.3 in the Lab Mode mixing CO_2 into a pure nitrogen atmosphere.

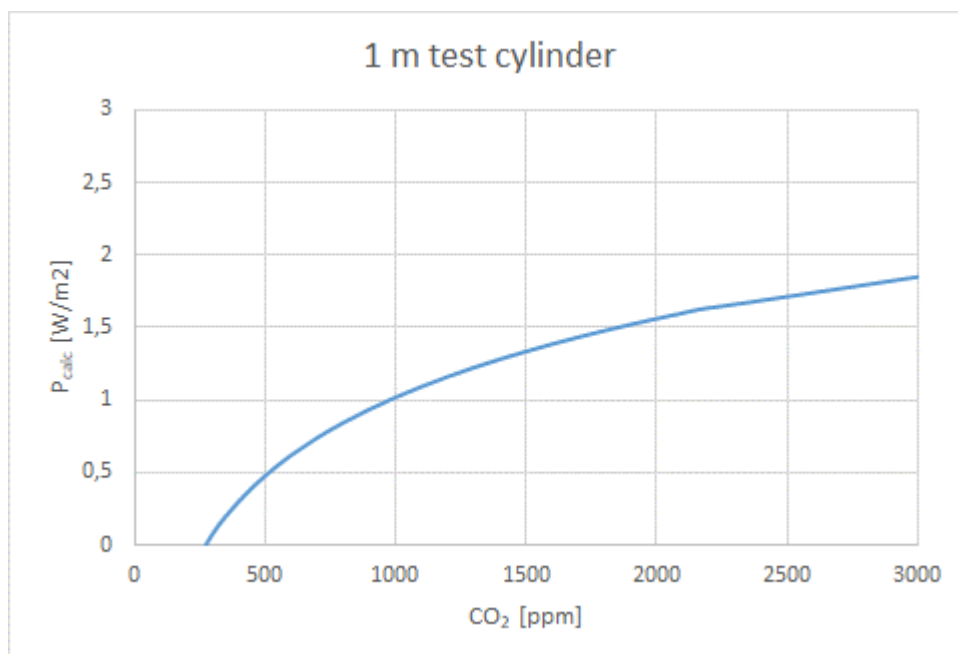From previous considerations we can estimate the back-radiation by the parametrization of Howard[11] (eqs 14, 15)

Low values of absorption length are outside the fit and measurement range of Howard but serve as extrapolations to estimate orders of magnitude. The trend in Fig.21 is indeed very similar to the measured values in Fig.20 and confirm the logarithmic behavior of the absorption.

Using the values plotted in Fig.20 we can estimate the fractional absorbance A_f for varying CO_2 concentrations in N2 atmospheres

$$\ln\left(\frac{I_0}{I_1}\right) = \epsilon \cdot c \cdot d \quad (19)$$

where c is the molar concentration (mol.m^{-3}) and d air column length (m). We use the Beer-Lambert law (13) function, where ϵ is the absorption coefficient of our test atmosphere to obtain

$$A_f = \frac{I_0 - I}{I} = \left(1 - e^{-\epsilon \cdot c \cdot d}\right) \quad (20)$$

Using (20) it is possible to find length of an air column at ground level conditions for saturation at given ppm CO_2.
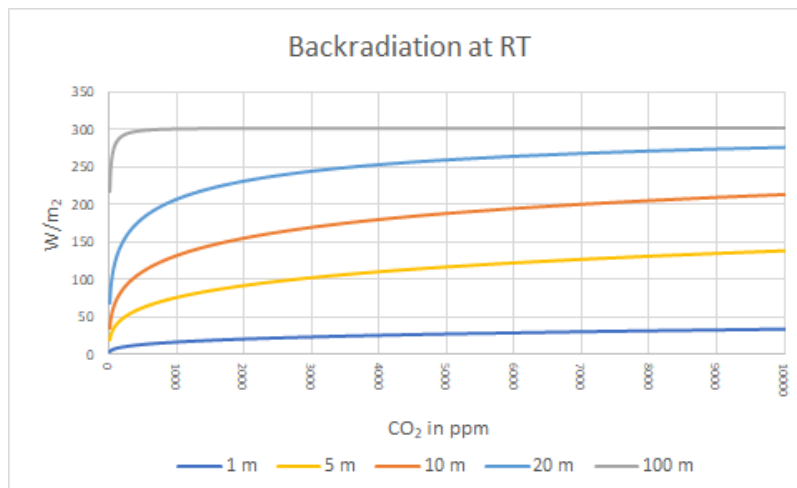

Figure 22: Calculated back-radiation for different long air columns at room temperature (RT)

In figure 23 we calculated the corresponding atmospheric thermal enhancement (ATE) when doubling the actual CO_2 concentration for an homogeneous atmosphere of 100 m thickness at 1 bar
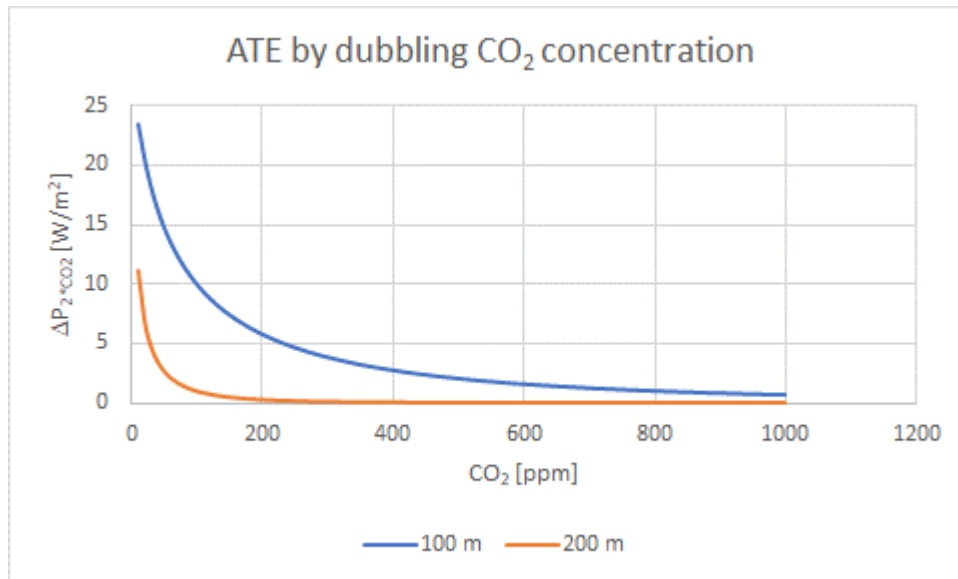
Figure 24: Calculated effect of CO_2 doubling on backscattered power in two air columns

The result shows a rapid reduction in ATE with increasing the length of the air columns. Applying this result to the real world means saturation in CO_2 concentration in respect to measurable thermal effects. This will be discussed in more detail in the next chapter.

Figure 25 was the result obtain in the so-called Outdoor Measurements against a black cloudless night sky. There is a clear indication that no measurable backscattering is observable when adding CO2 from 0 to 5000 ppm to the system. Eq. (9) with $\varepsilon_1 \sim 0.2$, $\varepsilon_2 < 0.2$ and $\beta \sim 0.02$ gives $\beta \varepsilon_1 \varepsilon_2 < 0.0004$ and therefore P = $\beta \varepsilon_1 \varepsilon_2 \sigma T_E^4 < 3 \times 10^{-2}$ W/m^2 = 3 μW/cm^2. The working power of the used PbSe Thorlabs detector with 1 cm^2 active area starts at 10 μW. For stronger GH gases it would be possible to exceed the detection limits and obtain a response. This was shown by using the Freon gas $C_2H_2F_4$ as shown in the next figure.
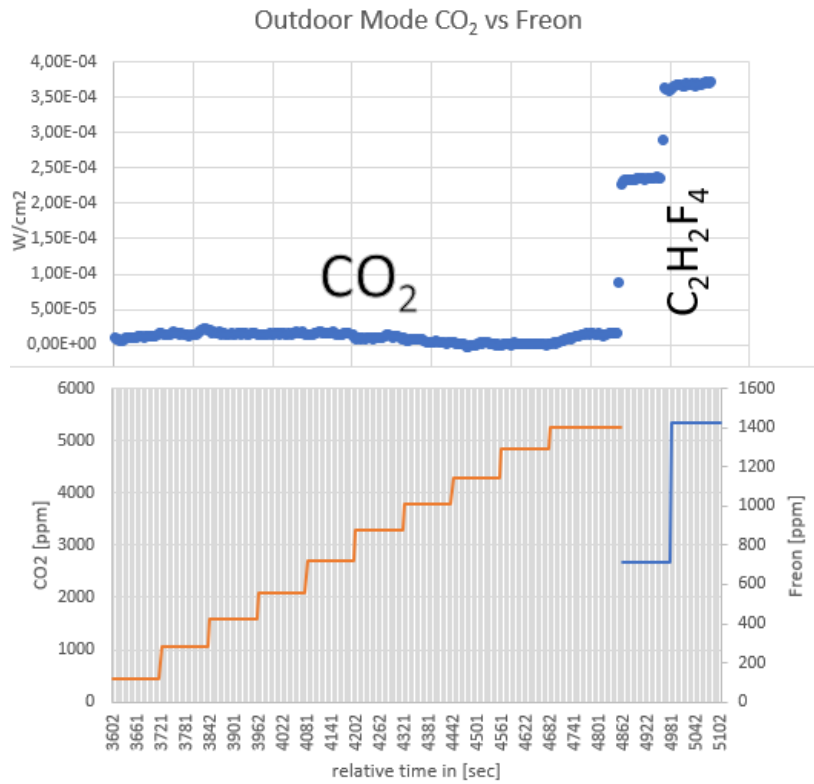
Figure 25: Outdoor Mode comparative measurement CO_2 and Freon ($C_2H_2F_4$)

The detector was indeed reacting, when $C_2H_2F_4$ Freon was added up to 1400 ppm. The measured absorbance of $C_2H_2F_4$ by NIST[19] is
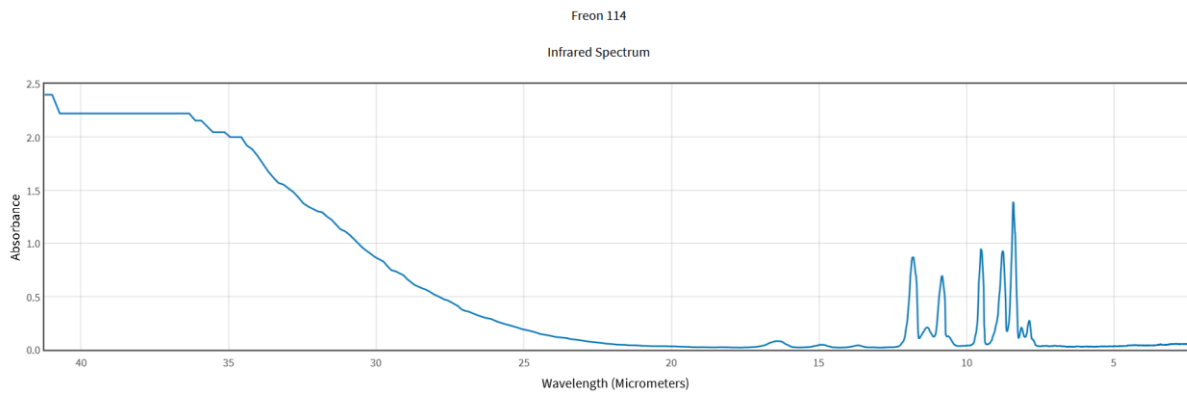

Figure 26: Absorbance of Freon ($C_2H_2F_4$) [19]

indeed up to 100 times stranger than CO_2 measured by the same institution[20]
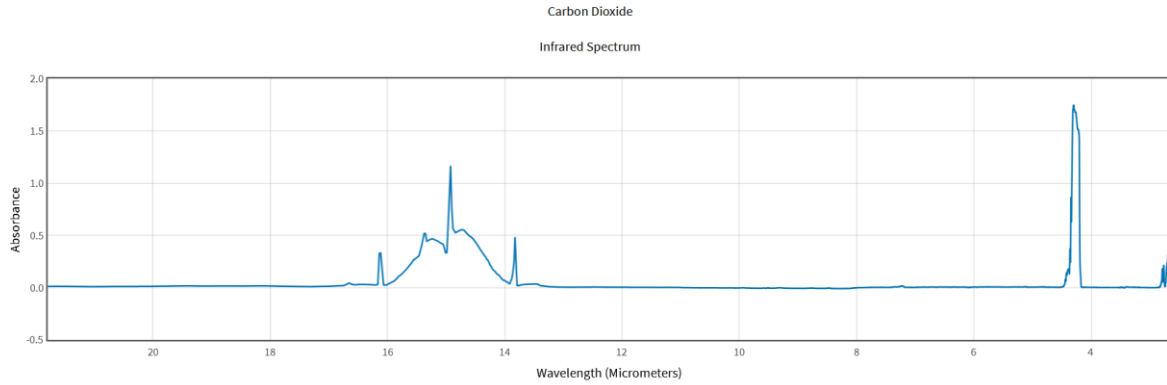
Figure 27: Absorbance of Carbon Dioxide (CO_2) [20]

IV.   Discussion

Atmospheric windows, especially the optical and infrared, affect the distribution of energy flows and temperatures within Earth's energy balance. The windows are themselves dependent upon clouds, water vapor, trace greenhouse gases, and other components of the atmosphere.

Out of an average 341 watts per square meter (W/m^2) of solar irradiance at the top of the atmosphere, about 161 W/m^2 reaches the surface via atmospheric windows and through clouds (albedo). IR absorption by the atmosphere and corresponding atmospheric heating leads to an equilibrium of 333 W/m^2 of back-radiation and outgoing LW surface radiation of 396 W/m^2 latent heat from evaporation (80 W/m^2) and other thermal losses (17 W/m^2). Our measurements fall in line with limitations to an increase of maximum 3W/m^2 back-radiation by doubling the CO_2 content from 400 to 800 ppm. This minor contribution should not exceed a temperature increase of more than 0.5°K a value, which is not within the range of significant impact for climatic changes and much lower than annual temperature variations in all regions of earth.
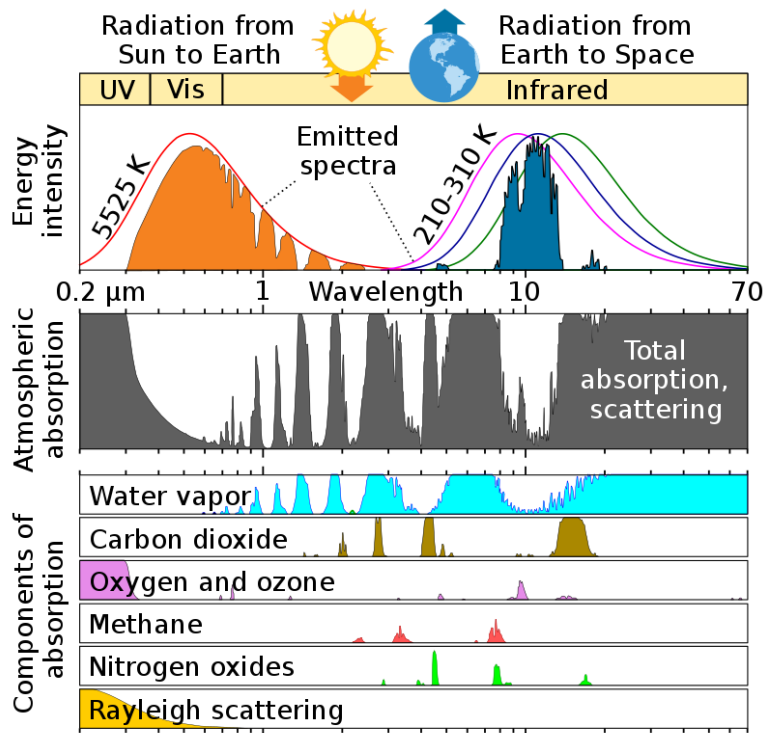
Figure 28: *The Atmospheric Window". National Oceanographic and Atmospheric Administration[14]. Retrieved 28 October 2022*

From Fig. 28 it should be obvious that only minor contributions can be obtained from the edges of the two prominent CO_2 windows. Water vapor is indeed the major absorber and other GH gases are not really relevant at their current concentrations. In a simplified picture, where we consider an atmosphere with uniform density corresponding to the surface density ρ = 1.2225 kgm^{-3} we obtain for an atmospheric air column weight of 10300 kgm^{-2} at a length of 8425 m. From our measurements and a simple Beer-Lambert model of such an air column we found in Fig. 18 already at 200m complete saturation at current CO_2 concentrations, without significant contributions to further ATE. Schildknecht[15] using similar arguments finds that doubling of the CO_2 content in air from 380 ppm to 760 ppm in one century an increase of $\Delta T \simeq 0.5$ °C, which corresponds well with the expected values of this and other works.

Our results should therefore contribute to previous accepted findings[2] which do not indicate any reason to cause climate run-aways by increased CO_2 contents. Ekholm[17] introduced the idea of fictitious atmospheric radiation levels due to CO_2 increase. According to him secular cooling of earth is the principal cause of variation in quantity of carbon dioxide in atmosphere. He explained how carbon dioxide is a key player in the greenhouse effect and how his conclusion was based on the earlier work of Fourier, Pouillet, Tyndall, and others. By their estimations a tripling of carbon dioxide levels will raise global temperatures 7 to 9 °C. An increase in carbon dioxide should heat high latitudes more than the tropics and create a warmer more uniform climate over the entire Earth. Hansen[18] testified this before Congress and raised public awareness of climate change. He started his career studying radiative transfer in Venus' atmosphere and applied this knowledge to Earth's atmosphere. He was claiming "The most powerful feedback is provided by water vapor". While this argument seems strong it must be questioned in light of paleoclimatic facts *e.g. higher temperatures in the Eemian interglacial period 120,000 years ago and in the Holstein interglacial period 5,000 to 15,000 years ago did not trigger a tipping point or a galloping greenhouse effect.* We first must

understand how it was possible to evaporate up to 100 m sea levels and to end up by glaciation over large areas of the landmasses without anthropogenic CO_2 emissions. And how could this energy by provided, if there was no temperature increase much higher than current measured values. Icecore data do not indicate such deviations from current temperature data.   We also need a better understanding of the usual power flow diagrams as published from the IPCC. Such diagrams are not in accordance with the basic laws of thermodynamics and actually indicate energy flows from cold to warm regions, which contradict the second law. It would be a great success of our efforts, if such questions could be reconsidered also in light of the results presented in this work.

V.   References

(1) Parliament, European. 2023. European Parliament. European Parliament. [Online] 11. 6 2023. https://www.europarl.europa.eu/news/de/headlines/society/20180706STO07407/fortschritte-der-eu-bei-der-verwirklichung-ihrer-klimaziele-infografik?at_campaign=20234-Green&at_medium=Google_Ads&at_platform=Search&at_creation=DSA&at_goal=TR_G&at_audience=&at_t.

(2) Wijngaarden, William Arie van and William Happer, "Dependence of Earth's Thermal Radiation on Five Most Abundant Greenhouse Gases", Atmospheric and Oceanic Physics (2020),   https://doi.org/10.48550/arXiv.2006.03098

(3) William Happer, Richard Lindzen, Comment and Declaration on the SEC's Proposed Rule "The Enhancement and Standardization of Climate-Related Disclosures for Investors," File No. S7-10-22, 87 Fed. Reg. 21334 (April 11,2022), https://www.sec.gov/comments/s7-10-22/s71022-20132171-302668.pdf

(4) Barrett, J. (2005). Greenhouse Molecules, Their Spectra and Function in the Atmosphere. Energy & Environment, 16(6), 1037–1045. https://doi.org/10.1260/095830505775221542

(5) James, I. (1994). Introduction to Circulating Atmospheres (Cambridge Atmospheric and Space Science Series). Cambridge: Cambridge University Press. doi:10.1017/CBO9780511622977

(6) https://www.acs.org/climatescience/atmosphericwarming/multilayermodel.html

(7) W. C. Swinbank, Quart. J. R. Met Soc., Vol 89, 381, July 1963, Pages 339-348

(8) Mark A. Goforth; George W. Gilchrist; Joseph D. Sirianni, Proceedings of SPIE - The International Society for Optical Engineering 4710, March 200

(9) David Tobin, Space Science and Engineering Center, University of Wisconsin-Madison, reprinted in A First Course In Atmospheric Radiation, By Grant W. Petty, p.223

(10) Angström, A. 1918 Smithsonian Inst., Misc. Coll., 65, 3
https://www.realclimate.org/images/Angstrom.pdf

(11) J. N. Howard, D. E. Burch, and Dudley Williams, "Infrared Transmission of Synthetic Atmospheres.* II. Absorption by Carbon Dioxide," J. Opt. Soc. Am. **46**, 237-241 (1956)

(12) C. Fröhlich, R. Philipona and C. Marty, "Untersuchung des Oberflächenstrahlungshaushaltes in den Alpen und im Vergleich zum schweizerischen Mittelland, 1998, vdf Hochschulverlag AG an der ETH Zürich

(13) Makhdoumi Akram, M., Nikfarjam, A., Hajghassem, H., Ramezannezhad, M., & Iraj, M. (2020). Low cost and miniaturized NDIR system for CO2 detection applications. Sensor Review, DOI 10.1108/SR-06-2019-0140

(14) Hermann Harde, OPEN JOURNAL OF ATMOSPHERIC AND CLIMATE CHANGE, Volume 1, Number 3, November 2014, 2374-3808, DOI: 10.15764/ACC.2014.03001

(15) Dieter Schildknecht, International Journal of Modern Physics B, Volume 34, Issue 30, id. 2050293, arXiv:2004.00708v2

(16) https://www.noaa.gov/jetstream/satellites/absorb

(17) Ekholm, Nils, 1901. On the Variations of the Climate of the Geological and Historical Past and Their Causes. *Quarterly Journal of the Royal Meteorological Society.* vol. 27. Pgs. 1-61

(18) Hansen, J., et al., Climate Impact of Increasing Atmospheric Carbon Dioxide. Science, 1981. 213(4511)

(19) https://webbook.nist.gov/cgi/cbook.cgi?ID=C76142&Type=IR-SPEC&Index=2

(20) https://webbook.nist.gov/cgi/cbook.cgi?ID=C124389&Units=SI&Type=IR-SPEC&Index=1#IR-SPEC